Cancer Science
Japanese Cancer Association JCA
Open Access

Ionizing radiation, inflammation, and their interactions in colon carcinogenesis in *Mlh1*-deficient mice

Takamitsu Morioka,[1,2,7] Tomoko Miyoshi-Imamura,[2,3,7] Benjamin J. Blyth,[2] Mutsumi Kaminishi,[2] Toshiaki Kokubo,[4] Mayumi Nishimura,[1,2] Seiji Kito,[4] Yutaka Tokairin,[5] Shusuke Tani,[2] Kimiko Murakami-Murofushi,[3] Naoki Yoshimi,[6] Yoshiya Shimada[1,2] and Shizuko Kakinuma[1,2]

[1]Radiation Effect Accumulation and Prevention Project, Fukushima Project Headquarters, National Institute of Radiological Sciences, Chiba; [2]Radiobiology for Children's Health Program, Research Center for Radiation Protection, National Institute of Radiological Sciences, Chiba, Japan; [3]Genetic Counseling Program, Graduate School of Humanities and Sciences, Ochanomizu University, Tokyo, Japan; [4]Research, Development and Support Center, National Institute of Radiological Sciences, Chiba, Japan; [5]Department of Esophageal and Surgery, Tokyo Medical and Dental University, Tokyo, Japan; [6]Department of Pathology and Oncology, Graduate School of Medical Science, University of the Ryukyus, Okinawa, Japan

Key words

Colon carcinogenesis, inflammation, Lynch syndrome, *Mlh1*, radiation

Correspondence

Shizuko Kakinuma, Radiobiology for Children's Health Program, Research Center for Radiation Protection, National Institute of Radiological Sciences, 4-9-1 Anagawa, Inage-ku, Chiba 263-8555, Japan.
Tel: +81-43-206-3160; Fax: +81-43-206-4138;
E-mail: skakinum@nirs.go.jp

Funding Information

Ministry of Education, Culture, Sports, Science, and Technology of Japan (22501009)

[7]These authors contributed equally to this work.

Received July 28, 2014; Revised December 5, 2014; Accepted December 11, 2014

Cancer Sci **106** (2015) 217–226

doi: 10.1111/cas.12591

Genetic, physiological and environmental factors are implicated in colorectal carcinogenesis. Mutations in the *mutL homolog 1* (*MLH1*) gene, one of the DNA mismatch repair genes, are a main cause of hereditary colon cancer syndromes such as Lynch syndrome. Long-term chronic inflammation is also a key risk factor, responsible for colitis-associated colorectal cancer; radiation exposure is also known to increase colorectal cancer risk. Here, we studied the effects of radiation exposure on inflammation-induced colon carcinogenesis in DNA mismatch repair-proficient and repair-deficient mice. Male and female *Mlh1*$^{-/-}$ and *Mlh1*$^{+/+}$ mice were irradiated with 2 Gy X-rays when aged 2 weeks or 7 weeks and/or were treated with 1% dextran sodium sulfate (DSS) in drinking water for 7 days at 10 weeks old to induce mild inflammatory colitis. No colon tumors developed after X-rays and/or DSS treatment in *Mlh1*$^{+/+}$ mice. Colon tumors developed after DSS treatment alone in *Mlh1*$^{-/-}$ mice, and exposure to radiation prior to DSS treatment increased the number of tumors. Histologically, colon tumors in the mice resembled the subtype of well-to-moderately differentiated adenocarcinomas with tumor-infiltrating lymphocytes of human Lynch syndrome. Immunohistochemistry revealed that expression of both p53 and β-catenin and loss of p21 and adenomatosis polyposis coli proteins were observed at the later stages of carcinogenesis, suggesting a course of molecular pathogenesis distinct from typical sporadic or colitis-associated colon cancer in humans. In conclusion, radiation exposure could further increase the risk of colorectal carcinogenesis induced by inflammation under the conditions of *Mlh1* deficiency.

Humans are exposed to multiple environmental carcinogens including genotoxic and non-genotoxic chemicals, heavy metals, inflammatory agents, and both UV and ionizing radiation. The leading factors contributing to human cancer are carcinogens in tobacco smoke followed by those in the diet, and inflammation. Heritable factors are estimated to account for 0–42% of cancers, depending on the organ,[1] in addition to the known genetic influence on the varying susceptibility of individuals to carcinogen exposures, including for radiation-induced cancer.[2] Combined exposures to environmental carcinogens in susceptible individuals in the population thus represent a high-risk scenario that warrants further investigation. Although interactions of ionizing radiation and genotoxin or hormone exposures have been studied,[3] little is known about interactions between ionizing radiation and inflammation in cancer-prone individuals.

Colorectal cancer (CRC) is the third most frequent malignancy worldwide[4] and is mostly sporadic. Yet heredity, mostly inherited defects in DNA mismatch repair (MMR), is a significant factor in 20–25% of cases.[5–7] The MMR pathway is responsible for repair of base mismatches and small insertions/deletions arising during DNA replication[8,9] and is important for maintaining genomic stability and preventing tumorigenesis.[10] Mutations in the MMR gene *mutL homolog 1* (*MLH1*) are involved in hereditary non-polyposis colorectal cancer, or Lynch syndrome.[11]

Inflammation is an important risk factor for gastrointestinal diseases and tumors,[12] with colitis-associated CRC the most serious long-term complication of inflammatory bowel disease.[13] Mild inflammation accelerates colon carcinogenesis in MMR-deficient mice (*Mlh1*$^{-/-}$, *Msh2*$^{-/-}$),[14,15] and can itself inactivate MMR through *Mlh1* promoter methylation.[16] Microsatellite instability (MSI) is also known to occur in colitis-associated CRC and dysplastic lesions in humans,[17] with one study revealing that 46% of colon neoplasms/lesions with a high degree of MSI showed hypermethylation of the *MLH1* gene.[18]

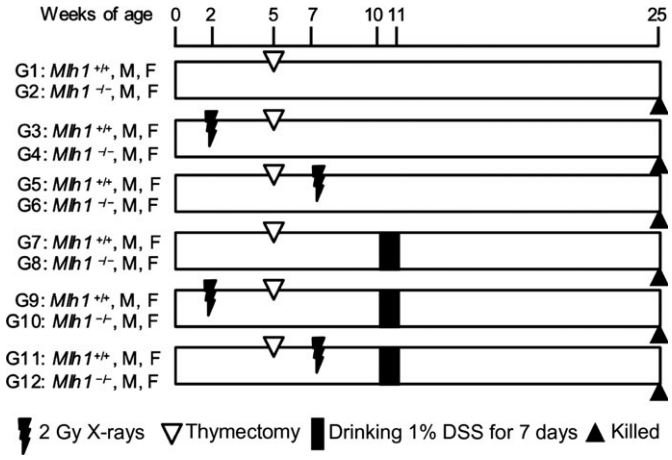

Fig. 1. Overview of the experimental design to ascertain the effects of radiation exposure on inflammation-induced colon carcinogenesis in DNA mismatch repair-proficient (*Mlh1*$^{+/+}$) and repair-deficient (*Mlh1*$^{-/-}$) mice. DSS, dextran sodium sulfate; F, female; M, male.

Colon cancer risk also increases following exposure to ionizing radiation,[19] now a consideration when evaluating adjuvant radiotherapy for abdominal cancers,[20,21] and justifying computed tomography colonography, a first-line screening modality to detect CRC. In addition to repairing endogenous damage, MMR is active in the response to radiation-induced DNA damage.[22,23] We previously showed a small but significant acceleration of intestinal tumor development after exposure to 2 Gy X-rays in 10-week-old *Mlh1*$^{-/-}$ mice, with no sensitivity observed in *Mlh1*$^{+/-}$ heterozygotes.[15,24] Yet, scarce data are available on the interaction between ionizing radiation and inflammation on colon carcinogenesis, particularly in conjunction with inherited MMR deficiency. Lynch syndrome patients are a subpopulation that may be at high risk for radiation-induced colon cancer, particularly in the context of chronic inflammation, warranting investigation for radiation protection purposes. Furthermore, the sensitivity of Lynch syndrome patients and mouse models of *Mlh1* deficiency provides an opportunity to observe interactions that are difficult to study in the wider population, but may have significant impact given the prevalence of both CRC and chronic inflammation.

Here, we examined the combined effect of ionizing radiation and induced inflammatory colitis on colon carcinogenesis in *Mlh1*$^{-/-}$ and control *Mlh1*$^{+/+}$ mice, and examined molecular pathogenesis through the expression of the CRC-associated proteins adenomatosis polyposis coli (Apc), β-catenin, p53, and p21.

Materials and Methods

Mice. Mice carrying a disrupted exon 4 of *Mlh1*, whose genetic background was >95% C57BL/6, were provided by Prof. Liskay (Oregon Health and Science University, Portland, OR, USA).[25] The *Mlh1* genotype was determined by PCR from mouse ear punch DNA as previously described.[24] Male and female mice were housed separately in stainless steel cages (4–5 mice per cage) with water and a standard laboratory diet (MB-1; Funabashi Farm, Chiba, Japan) provided *ad libitum*. They were maintained at 23 ± 2°C and 50 ± 10% humidity, on a 12:12 h light : dark cycle. All experiments were reviewed and approved by our institution's animal welfare committee.

Induction of inflammatory colitis. Treatment with dextran sodium sulfate (DSS) (molecular weight, 36 000–50 000; MP Biomedicals, Aurora, OH, USA) was used to induce colitis.[26,27] For induction of colitis, mice received 1% DSS in drinking water for 1 week when 10 weeks old. One cycle of the 1% DSS regimen, unlike repeated cycles of higher DSS doses, rarely leads to colon carcinogenesis and death in wild type (WT) mice.[26,28] Intake of distilled water (DW) or 1% DSS solution per cage (4–5 mice) was measured throughout the treatment periods. DW and DSS load (mL/day/mouse) was calculated.

Experimental design. A total of 226 *Mlh1*$^{+/+}$ and *Mlh1*$^{-/-}$ mice were divided into 12 experimental groups as shown in Figure 1. A dose of 2 Gy has been shown to accelerate colon carcinogenesis in susceptible mice models, yet the most sensitive time for radiation exposure differs between studies.[24,29] Therefore, the single whole-body irradiation of 2 Gy was given to mice at either 2 or 7 weeks old, to cover both of the observed peaks. X-ray irradiation was carried out using a Pantak X-ray generator (Pantak, East Haven, CT, USA) as previously described.[24] Most irradiated

Table 1. Effect of X-ray irradiation (2 Gy) and/or dextran sodium sulfate (DSS) on body weight (BW) in *Mlh1*$^{+/+}$ and *Mlh1*$^{-/-}$ mice

Group no.	Treatment	Genotype	BW, g	
			Male (no. of mice)	Female (no. of mice)
1	Untreated control	+/+	30.8 ± 1.3 (10)	22.3 ± 1.5 (10)
2		−/−	30.1 ± 2.1 (9)	22.4 ± 3.9 (8)
3	X-rays (2 weeks)	+/+	30.1 ± 2.4 (10)	24.2 ± 1.4** (10)
4		−/−	26.5 ± 3.3*,# (8)	22.2 ± 1.9# (9)
5	X-rays (7 weeks)	+/+	31.0 ± 1.2 (10)	24.4 ± 2.5* (10)
6		−/−	28.4 ± 1.8## (9)	21.9 ± 3.9 (8)
7	DSS (10 weeks)	+/+	31.5 ± 2.5 (10)	24.2 ± 1.7* (10)
8		−/−	28.6 ± 2.3# (9)	22.6 ± 2.8 (10)
9	X-rays (2 weeks)/DSS	+/+	29.9 ± 2.3 (10)	24.3 ± 2.7 (10)
10		−/−	27.2 ± 1.5**,## (9)	22.2 ± 2.7 (9)
11	X-rays (7 weeks)/DSS	+/+	28.9 ± 2.3* (10)	24.6 ± 3.8 (10)
12		−/−	26.2 ± 2.3**,# (10)	21.8 ± 2.1 (8)

The number of *Mlh1*$^{-/-}$ mice per group ranges from 8 to 10 for each sex because a small number of mice died due to thymectomy or DSS treatment. Data are shown as the mean ± SD. *$P < 0.05$, **$P < 0.01$, significant difference from no treatment group of same genotype by an unpaired Student's *t*-test. #$P < 0.05$, ##$P < 0.01$, significant difference from *Mlh1*$^{+/+}$ mice treated with same condition by an unpaired Student *t*-test.

Table 2. Intake of dextran sodium sulfate (DSS) and distilled water (DW) in *Mlh1*$^{+/+}$ and *Mlh1*$^{-/-}$ mice

	Genotype	Male	Female
DSS	+/+	3.20 ± 0.09*	2.70 ± 0.04
	−/−	3.33 ± 0.16*	2.59 ± 0.03
DW	+/+	3.63 ± 0.07*	3.30 ± 0.05
	−/−	3.63 ± 0.07*	3.34 ± 0.03

Data are shown as the mean ± SE (mL). *$P < 0.05$, significant difference from female mice of same genotype by an unpaired Student's *t*-test.

Mlh1$^{-/-}$ mice develop thymic lymphomas before colon tumors arise, which makes it difficult to quantitatively assess the role of *Mlh1* deficiency in colon carcinogenesis. Therefore, in this experiment, thymectomy was carried out at 5 weeks old to exclude the confounding factor of thymic lymphoma in mice of all groups. All mice were weighed before being killed under terminal isoflurane anesthesia when 25 weeks old.

Histopathological examination. After death, the colons were harvested and the mucosal layer spread out over filter paper to expose any lesions protruding into the lumen. The flattened tissues were then fixed with 10% neutral-buffered formalin for 24 h and then examined closely for lesions. Colon lesions were then stained with H&E for histological analysis, with mucosal dysplasia and neoplasms diagnosed according to previously established criteria.[30–32]

Immunohistochemical staining. Serial 4-μm-thick paraffin sections were used for immunohistochemical examination to determine the expression of Apc, β-catenin, p53, and p21 proteins. These sections were stained with primary antibodies at the following dilutions: 1:50 for Apc (polyclonal; Abcam, Tokyo, Japan), 1:100 for β-catenin (monoclonal; BD Transduction Laboratories, Lexington, KY, USA), 1:500 for p53 (polyclonal; Novocastra Laboratories, Newcastle, UK), and 1:500 for p21 (polyclonal; Santa Cruz Biotechnology, Santa Cruz, CA, USA). Standard protocols for immunohistochemistry were followed as described previously.[15]

Harvesting DNA from colon lesions by laser capture microdissection. β-catenin- and p53-positive focal areas and adjacent normal mucosa were isolated from the immunostained tissues by laser capture microdissection (MMI CellCut; Molecular Machines and Industries, Eching, Germany) and collected onto the adhesive cap of the provided 500-μL microcentrifuge tubes. DNA was extracted using the QIAmp DNA Micro kit (Qiagen, Hilden, Germany) according to their specific protocol for extraction of genomic DNA from laser capture microdissection tissues.

Mutation analysis of β-*catenin* and *p53* genes. The PCR primers were designed to amplify exon 3 of β-catenin, which encodes the GSK-3β phosphorylation sites, a known mutation hotspot. The sequences of the primers were as follows: for exon 3, ctnnb1-F (5′-GGA GTT GGA CAT GGC CAT GG-3′) and ctnnb1-R (5′-TCA ACA TCT TCT TCC TCA GG-3′). The PCR primers to amplify p53 exons 6, 7, 8, and 9 were designed, giving coverage of the coding region for the DNA-binding domain. The sequences of the primers were as follows: for exon 6, E6-1F (5′-TCC CGG CTT CTG ACT TAT TC-3′) and E6-1R (5′-TGC CTG TCT TCC AGA TAC TCG-3′), E6-2F (5′-CGG GTG GAA GGA AAT TTG TA-3′) and E6-2R (5′-AAG ACG CAC AAA CCA AAA CA-3′); for exon 7, E7-1F (5′-GTA GGG AGC GAC TTC ACC TG-3′) and E7-1R (5′-CCC CAT GCA GGA GCT ATT AC-3′), E7-2F (5′-TAC CAC CAT CCA CTA CAA GTA CA-3′) and E7-2R (5′-CTA CCA CGC GCC TTC CTA C-3′); for exon 8, E8-F2 (5′-TGC TGG TCC TTT TCT TGT CC-3′) and E8-R2 (5′-TGA AGC TCA ACA GGC TCC TC-3′); for exon 9, E9-F (5′-GGA GGA GCC TGT TGA GCT TC-3′) and E9-R (5′-ATG CGA GAG ACA GAG GCA AT-3′). The PCR products were directly sequenced using a BigDye Terminator Version 3.1 Cycle Sequencing Kit (Applied Biosystems, Foster City, CA, USA) and ABI PRISM 3100 Genetic Analyzer (Applied Biosystems) following the manufacturer's protocol.

Statistical evaluation of data. All statistical analyses were carried out using R version 2.15.0 software function nlm (http: www.r-project.org). An unpaired Student's *t*-test was used to analyze average body weight (BW) and for intake of DW and 1% DSS. Fisher's exact probability test was used to analyze the incidence of colon lesions; the Kruscal–Wallis test with Steel–Dwass multiple comparisons method and the Mann–Whitney *U*-test were used to analyze the multiplicity of

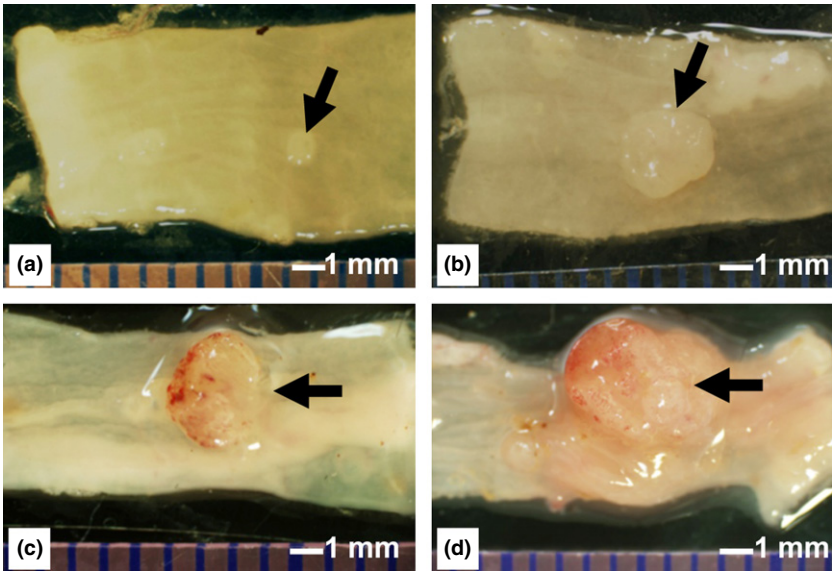

Fig. 2. Macroscopic view of representative colon lesions from *Mlh1*$^{-/-}$ mice treated with X-ray irradiation and dextran sodium sulfate (DSS) alone or in combination. (a) X-rays (7 weeks) + DSS, female (arrow, single small protruded lesion). (b) X-rays (7 weeks) + DSS, male (arrow, single sessile polyp without hemorrhage). (c) DSS only, female (arrow, single large sessile polyp with hemorrhage). (d) X-rays (2 weeks) + DSS, male (arrow, single large sessile polyp with hemorrhage).

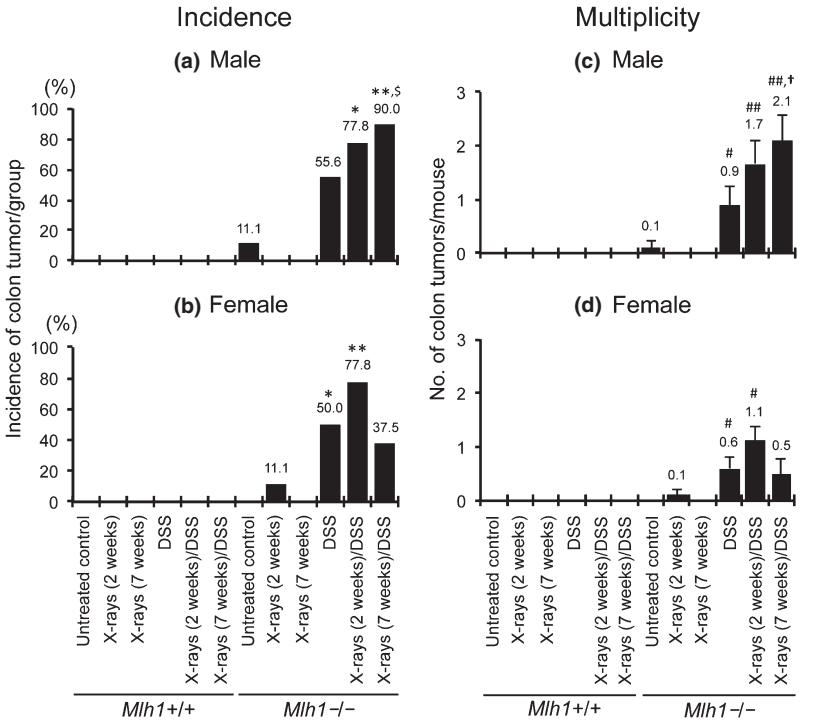

Fig. 3. Incidence and multiplicity of colon lesions in *Mlh1*$^{+/+}$ and *Mlh1*$^{-/-}$ mice treated with X-ray irradiation or dextran sodium sulfate (DSS) alone or in combination. Incidence of colon lesions (number of mice with at least one colon lesion compared to total number of mice) is shown as a percentage for each group (a, b) and the multiplicity (number of colon lesions per mouse) is shown as the mean ± SE for each group (c, d). $*P < 0.05$, $**P < 0.01$ versus control, Fisher's exact probability test. $\#P < 0.05$, $\#\#P < 0.01$ versus control, Kruscal–Wallis test with Steel–Dwass multiple comparisons method. $\$P < 0.05$ versus treatment-matched female mice, Fisher's exact probability test. $\dagger P < 0.05$ versus treatment-matched female mice, Mann–Whitney *U*-test.

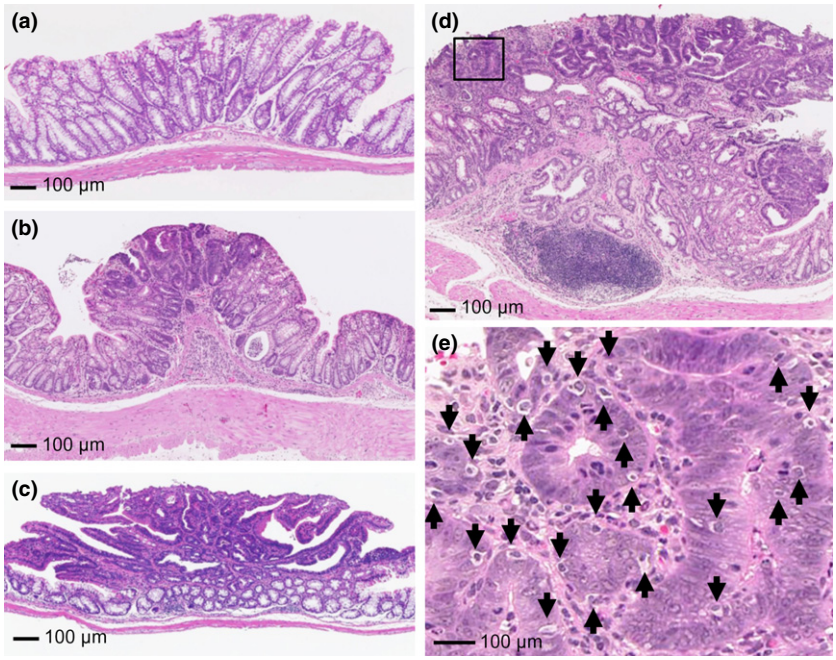

Fig. 4. Histopathology of colon lesions in *Mlh1*$^{-/-}$ mice (H&E) treated with X-ray irradiation or dextran sodium sulfate alone or in combination. (a) Hyperplasia (group 10, female). (b) Dysplasia (group 12, male). (c) Tubular adenoma (group 10, female). (d) Well-differentiated tubular adenocarcinoma (group 12, male). (e) Magnified view of the boxed area in (d). Numerous tumor-infiltrating lymphocytes are present in the neoplastic epithelium and stroma (arrows).

colon lesions. The results were considered significant at $P < 0.05$.

Results

Changes in BW. Although BW was significantly lower in all treated male mice on the *Mlh1*$^{-/-}$ background compared to treatment-matched WT males, only the combined exposures and X-rays at 2 weeks old caused a significant reduction below the weight of the *Mlh1*$^{-/-}$ control males (Table 1). Only DSS combined with irradiation at 7 weeks caused a significant reduction in BW for WT males compared to the WT control males. In contrast, female mice on the *Mlh1*$^{-/-}$ background showed no changes in BW, whereas the controls showed the lowest BW for WT females, with the three single treatments each causing a significant increase in weight at 25 weeks old.

Intake of DSS and DW. The mean daily intake of DSS and DW for mice of each *Mlh1* genotype is shown in Table 2. Although female mice drank less water than males, males and females of both genotypes drank less when DSS was present, and the drop in intake was more pronounced in females, leading to a lower relative intake of DSS in females compared to males.

Macroscopic view of colon lesions induced by single and combined exposure to X-rays and DSS. The typical gross appearance of colon lesions, which varied in size from 0.5 to 6 mm in

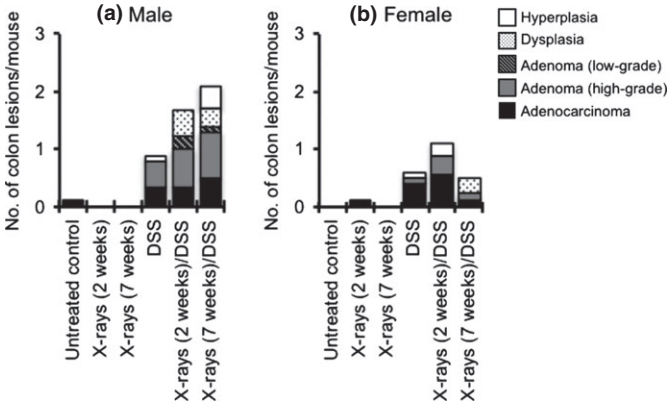

Fig. 5. Histological classification of colon lesions in male (a) and female (b) *Mlh1*$^{-/-}$ mice treated with X-ray irradiation or dextran sodium sulfate (DSS) alone or in combination.

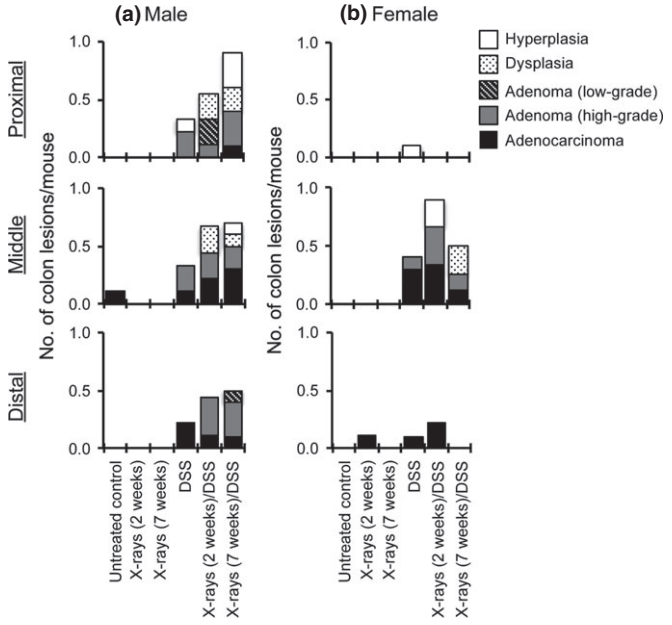

Fig. 6. Distribution of lesions in the colon in male (a) and female (b) *Mlh1*$^{-/-}$ mice treated with X-ray irradiation or dextran sodium sulfate alone or in combination.

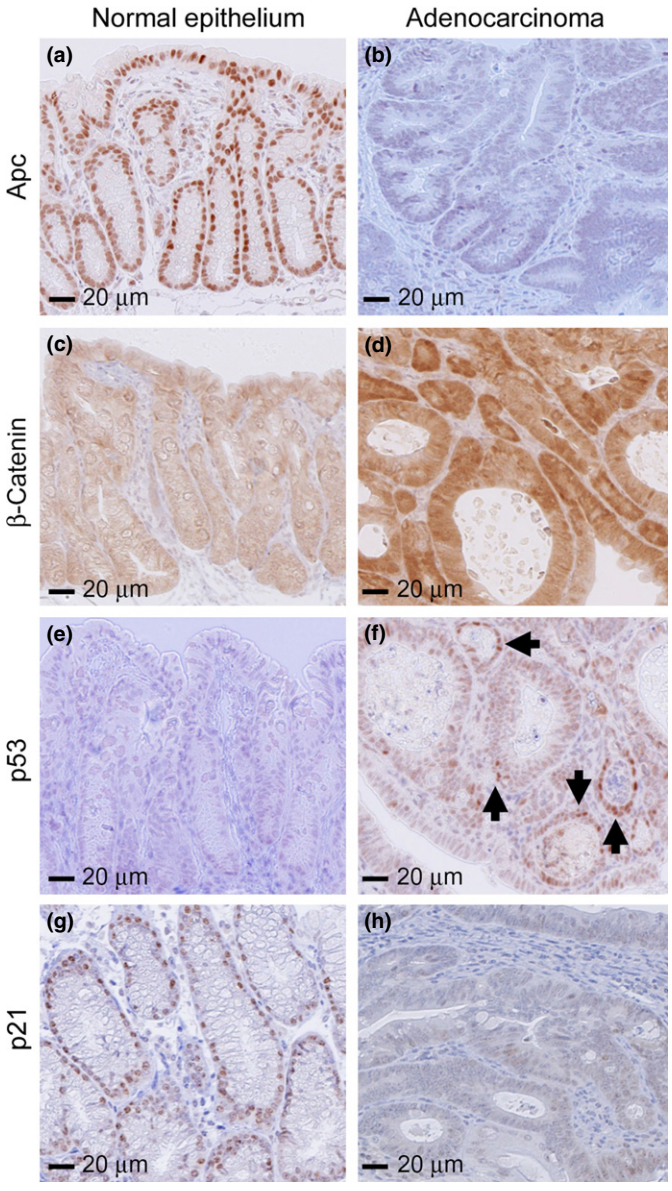

Fig. 7. Immunohistochemical analysis of adenomatosis polyposis coli (Apc), β-catenin, p53, and p21 expression in normal epithelium (a, c, e, and g) and adenocarcinoma (b, d, f, and h) from *Mlh1*$^{-/-}$ mice treated with X-ray irradiation and dextran sodium sulfate (group 10 or 12). Arrows indicate strong expression of p53 in atypical glands.

diameter, is shown in Figure 2. All lesions were sessile types and protruded into the lumen as a polyp (Fig. 2b–d) or plaque (Fig. 2a). The large lesions, but no small lesions, had hemorrhage on part of the upper surface (Fig. 2c,d). No other tumors developed during the experimental period.

Combination of X-rays and DSS enhanced colon lesions in *Mlh1*$^{-/-}$ mice. We first evaluated the incidence and multiplicity of colon lesions induced by the combinations of radiation exposure and DSS treatment, as shown in Figure 3. No colon lesions were observed in WT mice with any treatment. A single colon lesion was observed in an untreated male and one in a female exposed to X-rays at 2 weeks old, an indication of the low baseline frequency without DSS induction. All the remaining lesions arose following DSS alone or in combination with radiation at 2 or 7 weeks old, with an incidence in males of 55.6%, 77.8%, and 90%, respectively. The increase in the incidence in males receiving the combined X-rays and DSS treatments above untreated controls reached statistical significance, but not in those given DSS alone. In females, both DSS alone and in combination with X-ray irradiation at 2 weeks old significantly increased incidence above that observed in untreated females, with a higher frequency when the DSS followed irradiation at 2 weeks old. Unlike the males, no additional lesions compared to DSS alone were observed in females after irradiation at 7 weeks old. Although the number of mice available per group did not permit a formal test of synergy between the two treatments, the near complete penetrance in males given DSS combined with irradiation at 7 weeks old was remarkable, and the putative additional colon lesions observed across the four combined-exposure groups exceeded what might have been expected from even an additive effect from the X-ray-induced incidence.

Multiplicity of colon lesions largely mirrored the trends observed in the incidence data, and was consistent with the

Table 3. Immunohistochemical staining of adenomatosis polyposis coli (Apc), β-catenin, p53, and p21 in colon lesions in *Mlh1*$^{-/-}$ mice treated with X-ray irradiation and/or dextran sodium sulfate (DSS)

Treatment Colon lesions	Apc			β-catenin			p53			p21		
	Nucleus			Membrane	Cytoplasm/nucleus		Nucleus			Nucleus		
	–	+	++	+	+	++	–	+	++	–	+	++
Untreated control												
Normal epithelium	0/1 (0)	0/1 (0)	1/1 (100)	1/1 (100)	0/1 (0)	0/1 (0)	1/1 (100)	0/1 (0)	0/1 (0)	0/1 (0)	0/1 (0)	1/1 (100)
Hyperplasia	–	–	–	–	–	–	–	–	–	–	–	–
Dysplasia	–	–	–	–	–	–	–	–	–	–	–	–
Adenoma	–	–	–	–	–	–	–	–	–	–	–	–
Adenocarcinoma	0/1 (0)	0/1 (0)	1/1 (100)	0/1 (0)	0/1 (0)	1/1 (100)	1/1 (100)	0/1 (0)	0/1 (0)	0/1 (0)	0/1 (0)	1/1 (100)
X-rays (2 weeks)												
Normal epithelium	0/1 (0)	0/1 (0)	1/1 (100)	1/1 (100)	0/1 (0)	0/1 (0)	1/1 (100)	0/1 (0)	0/1 (0)	0/1 (0)	0/1 (0)	1/1 (100)
Hyperplasia	–	–	–	–	–	–	–	–	–	–	–	–
Dysplasia	–	–	–	–	–	–	–	–	–	–	–	–
Adenoma	–	–	–	–	–	–	–	–	–	–	–	–
Adenocarcinoma	0/1 (0)	0/1 (0)	1/1 (100)	0/1 (0)	0/1 (0)	1/1 (100)	0/1 (0)	1/1 (100)	0/1 (0)	0/1 (0)	1/1 (100)	0/1 (0)
DSS												
Normal epithelium	0/10 (0)	0/10 (0)	10/10 (100)	14/14 (100)	0/14 (0)	0/14 (0)	14/14 (100)	0/14 (0)	0/14 (0)	0/14 (0)	0/14 (0)	14/14 (100)
Hyperplasia	0/1 (0)	0/1 (0)	1/1 (100)	2/2 (100)	0/2 (0)	0/2 (0)	2/2 (100)	0/2 (0)	0/2 (0)	0/2 (0)	2/2 (100)	0/2 (0)
Dysplasia	–	–	–	–	–	–	–	–	–	–	–	–
Adenoma	0/3 (0)	0/3 (0)	3/3 (100)	2/5 (40)	2/5 (40)	1/5 (10)	2/5 (40)	3/5 (60)	0/5 (0)	1/5 (20)	4/5 (80)	0/5 (0)
Adenocarcinoma	1/6 (16.7)	0/6 (0)	5/6 (88.3)	0/7 (0)	3/7 (42.9)	4/7 (57.1)	1/7 (14.3)	6/7 (85.7)	0/7 (0)	1/7 (14.3)	6/7 (85.7)	0/7 (0)
X-rays (2 weeks)/DSS												
Normal epithelium	0/20 (0)	0/20 (0)	20/20 (100)	25/25 (100)	0/25 (0)	0/25 (0)	25/25 (100)	0/25 (0)	0/25 (0)	0/22 (0)	0/22 (0)	22/22 (100)
Hyperplasia	–	–	–	2/2 (100)	0/2 (0)	0/2 (0)	2/2 (100)	0/2 (0)	0/2 (0)	0/1 (0)	1/1 (100)	0/1 (0)
Dysplasia	0/4 (0)	0/4 (0)	4/4 (100)	4/4 (100)	0/4 (0)	0/4 (0)	4/4 (100)	0/4 (0)	0/4 (0)	1/4 (25)	3/4 (75)	0/4 (0)
Adenoma	0/8 (0)	3/8 (37.5)	5/8 (62.5)	3/11 (27.3)	0/11 (0)	8/11 (72.7)	6/11 (54.5)	5/11 (45.5)	0/11 (0)	3/9 (33.3)	6/9 (66.7)	0/9 (0)
Adenocarcinoma	0/8 (0)	6/8 (75)	2/8 (25)	0/8 (0)	0/8 (0)	8/8 (100)	4/8 (50)	4/8 (50)	0/8 (0)	3/8 (37.5)	5/8 (62.5)	0/8 (0)
X-rays (7 weeks)/DSS												
Normal epithelium	0/15 (0)	0/15 (0)	15/15 (100)	23/23 (100)	0/23 (0)	0/23 (0)	23/23 (100)	0/23 (0)	0/23 (0)	0/23 (0)	0/23 (0)	23/23 (100)
Hyperplasia	–	–	–	3/3 (100)	0/3 (0)	0/3 (0)	3/3 (100)	0/3 (0)	0/3 (0)	0/3 (0)	3/3 (100)	0/3 (0)
Dysplasia	0/1 (0)	1/1 (100)	0/1 (0)	2/4 (50)	1/4 (25)	1/4 (25)	1/4 (25)	3/4 (75)	0/4 (0)	1/4 (25)	3/4 (75)	0/4 (0)
Adenoma	1/8 (12.5)	5/8 (62.5)	2/8 (25)	2/10 (20)	2/10 (20)	6/10 (60)	2/10 (20)	7/10 (70)	1/10 (10)	1/10 (10)	9/10 (90)	0/10 (0)
Adenocarcinoma	0/6 (0)	2/6 (33.3)	4/6 (66.7)	0/6 (0)	0/6 (0)	6/6 (100)	2/6 (33.3)	3/6 (50)	1/6 (16.7)	3/6 (50)	3/6 (50)	0/6 (0)

Staining graded as: –, negative; +, positive; ++, strongly positive. Percentages are shown in parentheses. –, Without colon lesions.

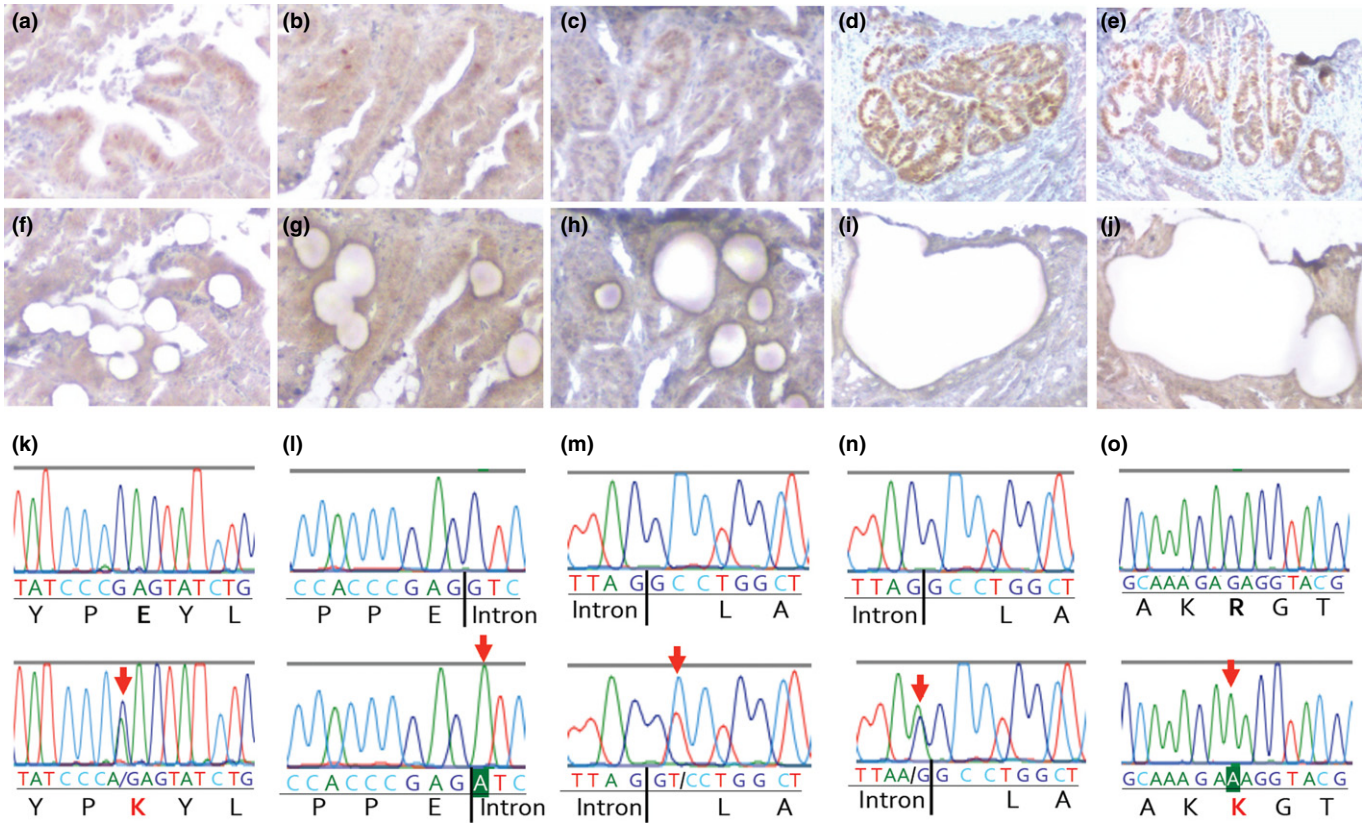

Fig. 8. Distinct strong positive p53 staining areas were observed in one adenocarcinoma (a–c) and one adenoma (d,e) induced by combined X-ray and dextran sodium sulfate (DSS) exposure in *Mlh1*$^{-/-}$ mice (group 12). Re-imaging after microdissection shows the isolated cells from the same field above (f–j). For each region, p53 sequencing results are shown corresponding to the fields above (k–o) in the lower trace, compared to the upper trace sequenced from adjacent normal tissue. Red arrows indicate mutated sites and red letters show amino acid substitutions.

various treatments influencing the probability of colon lesions for each mouse rather than increasing the number of colon lesions in the susceptible mice. The difference in multiplicity between males and females was due to a consistently lower number of colon lesions found per tumor-bearing mouse in females, despite a similar incidence of colon lesions between the sexes.

Histopathological findings of colon lesions induced by single and combined exposure to X-rays and DSS. Mucosal hyperplasia was slightly elevated above the mucosal surface and consisted of glandular hyperplasia. The glands were lined with hyperplastic basophilic epithelium with goblet cell differentiation; there was no cellular atypia (Fig. 4a). Dysplasia consisted of one or more glands lined with hyperchromatic atypical columnar epithelium with closely packed nuclei (Fig. 4b). Dysplastic cells showed loss of normal progression from germinal to fully differentiated cells, and goblet cells were not seen. Tubular adenoma (Fig. 4c) and tubular adenocarcinoma (Fig. 4d) were seen as endophytic lesions in the mucosa. These tumors consisted of irregular-sized glands lined with dysplastic glandular epithelium with many tumor-infiltrating lymphocytes (TIL) (Fig. 4e). In adenocarcinoma, there was obvious invasion of the muscularis mucosa by neoplastic glands (Fig. 4d).

Histological examination of colon lesions indicated that combined exposure of male *Mlh1*$^{-/-}$ mice to X-rays and DSS increased the number of low-grade adenomas, dysplasia, and hyperplasia compared with DSS treatment alone (Fig. 5). In females, compared with DSS treatment alone, combined exposure to X-rays at 2 weeks old also increased the number of high-grade adenomas and hyperplasia. In contrast, the failure to observe an enhanced incidence of colon lesions in females with combined exposure to DSS and X-rays at 7 weeks old was due to an unexplained decrease in low- and high-grade adenomas and carcinomas.

Figure 6 indicates the distribution of colon lesions in the distal, middle, and proximal areas of the colon. Colon lesions were distributed in all three segments at similar rates in males, whereas in females colon lesions were mainly observed in the middle area of the colon. Low- and high-grade adenomas and adenocarcinomas were mainly distributed in the distal and middle areas in both male and female *Mlh1*$^{-/-}$ mice. However, low-grade lesions such as hyperplasia and dysplasia were predominantly distributed in the proximal area in male *Mlh1*$^{-/-}$ mice.

Immunohistochemical staining of Apc, β-catenin, p53, and p21 in colon lesions of *Mlh1*$^{-/-}$ mice. We analyzed the expression of Apc, p53, β-catenin, and p21 proteins in colon lesions of *Mlh1*$^{-/-}$ mice by immunohistochemistry (Fig. 7, Table 3). Apc, which was strongly expressed in the nuclei of normal mucosal epithelium (Fig. 7a), became faint in adenomas and adenocarcinomas (Fig. 7b), suggesting that inactivation of Apc protein is a late event in colon carcinogenesis in this mouse model. The levels of β-catenin protein were concentrated in membranes of normal epithelium (Fig. 7c) but could be found in the nuclei and cytoplasm of adenomas and adenocarcinoma cells (Fig. 7d). Positivity of strong nuclear β-catenin staining was 84% and 75% of adenomas and adenocarcinomas from mice given DSS combined with irradiation at 2 and 7 weeks old, respectively, higher than in

tumors from mice given DSS alone (42%). This also indicated that nuclear localization of β-catenin is a late phenomenon. Weak, diffuse expression of p53 was frequently observed in adenomas (57.7%) and adenocarcinomas (60.9%), with strong expression of p53 in some atypical glands only rarely observed in adenomas (1/10, 10%) and adenocarcinomas (1/6, 16.7%) (Fig. 7f) and no expression observed in normal epithelium (Fig. 7e). The expression level of p21 protein was reduced in most colon tumors compared to normal colon epithelium (Fig. 7g,h). Taken together, these results indicate that dysregulation of Apc, p53, and β-catenin were all late events in colon carcinogenesis in $Mlh1^{-/-}$ mice treated with X-rays and DSS exposure.

Mutation analysis of β-*catenin* and *p53* genes. Exon 3 of the β-*catenin* gene was sequenced from a total 36 β-catenin-positive lesions (1 dysplastic lesion, 15 adenomas, and 20 adenocarcinomas), yet no mutations were observed in this mutation hotspot region (data not shown). In addition to the colon lesions with positive staining for p53, there were two mice with colon tumors showing regions of strong p53-positivity (one with a strong p53-positive adenocarcinoma and the other with a strong p53-positive adenoma). Within these two tumors, DNA was extracted from various regions showing strong p53 immunostaining (Fig. 8a–e). In the adenocarcinoma, three separate regions of strong p53 staining were sampled (Fig. 8f–h) each showing independent p53 mutations (Fig. 8k–m). The mutations were all single-nucleotide substitutions: the first leading to a Q201K amino acid substitution (homologous to the human Q204K mutation observed in Hodgkin's disease;[33] a GT>AT change at the splice donor site of intron 6, which has been shown at the equivalent site in a human case to create a six amino acid insertion;[34] and a seemingly silent change at the start of exon 6. In the adenoma, three regions of strong p53 staining were sampled (Fig. 8i,j) with two of them harboring single-nucleotide substitutions in the analyzed area of the DNA binding domain (Fig. 8n,o). Interestingly, the first was also at the start of exon 6, but this time an AG>AA change at the splice acceptor site. As mutations at this acceptor site (and at the position preceding it) have been shown in human cancer to result in omission of exon 6, yielding a premature stop codon,[35,36] it is likely that both this mutation and the otherwise silent change in the adenocarcinoma produce aberrantly spliced p53 protein. The second mutation in the adenoma is predicted to result in an R303K substitution (equivalent to R306K in human p53). Aberrant p53 DNA sequences were not detected in two moderately p53 stained areas adjacent to the strong p53 staining tumor regions, four p53-postive areas from other moderately staining lesions, nor normal non-staining tissue adjacent to each of the five lesions studied in total (data not shown).

Discussion

We have shown that combined exposure to radiation and mild inflammation could potentiate colon carcinogenesis under MMR-deficient conditions, although the trend was more pronounced in male mice. Dextran sodium sulfate (DSS)-induced cancer in WT mice typically requires long exposure periods or multiple cycles of DSS treatment, yet in $Mlh1^{-/-}$ mice, 1% DSS exposure for 1 week induces colon neoplasms with short latency (by 25 weeks old).[15] DSS treatment is able to promote tumors in WT mice when combined with initiating chemical treatments,[37–39] but did not promote tumors in irradiated WT mice, perhaps due to insufficient dose.[40] In contrast, even a single 2 Gy dose combined with DSS induced colon tumors in MMR-deficient mice, consistent with other evidence supporting synergistic mutagenicity of radiation in DNA repair-deficient cells.[23,41]

A subset of human CRC with MMR pathway defects are characterized by high levels of genome-wide MSI.[42] It is estimated that 15% of sporadic CRC exhibits MSI whereas the remaining cases are primarily attributed to an early loss of APC by chromosomal instability and/or mutation leading to adenoma by upregulation of β-catenin,[43] with rare progression to carcinoma (usually marked by eventual inactivation of P53),[44] or colitis-associated CRC, marked by early loss of P53 in mucosa subjected to prolonged inflammation,[45] leading to increasing dysplasia before ultimate loss of APC and progression to carcinoma.[46]

Tumors with inherited (Lynch syndrome) and acquired inactivation (usually through promoter methylation) of the MMR pathway (sporadic CRC) are postulated to follow different tumorigenic pathways.[47] In Lynch syndrome, CRCs are thought to arise by stochastic mutations in a constellation of genes as a result of disrupted DNA repair, with a number of genes with unstable short nucleotide repeats thought to drive transformation.[46] Lynch syndrome CRCs typically progress from adenomas, which morphologically tend to show features associated with increased risk of progression[48–50] and, unlike sporadic CRC, show a very high probability of transition to carcinoma.[44]

Lynch syndrome carcinomas are characterized by the presence of TIL and Crohn's-like lymphocytic reactions.[51–54] They fall into three main groups, the most common of which is moderate to well-differentiated, well-circumscribed mucinous carcinoma often associated with adjacent signet ring cells, mucinous cells with extracellular mucin, and tubulovillous or villous adenomatous remnants.[55,56] The second type is poorly differentiated adenocarcinoma with a medullary growth pattern that is well circumscribed and lacks abundant desmoplastic stroma.[56] The third type is well to moderately differentiated adenocarcinoma with occasional serrated polyps.[55,57]

The principal pathological characteristics of colon lesions induced here by combined exposure to X-rays and DSS in $Mlh1^{-/-}$ mice were dysplasia, adenoma with low- and high-grade dysplasia, and well-differentiated adenocarcinoma with TIL, akin to the well-differentiated adenocarcinoma with TIL seen in human Lynch syndrome. Aberrant APC, β-catenin, and P53 were identified mainly in the more advanced lesions, suggesting that these were late events, distinct from the early causal roles of APC or P53 inactivation in the two canonical pathways in human sporadic CRC or colitis-associated cancer. Histologically, the tumors induced by the combination of X-rays and DSS were similar to those in mice treated with DSS alone, although they tended to show higher expression of β-catenin and p53. The emergence of multifocal areas of inactivated p53 due to independent mutation events within tumors induced by the combined treatment may be a sign of increased tumor progression. The lack of β-catenin mutations might suggest that the increased levels of β-catenin staining are secondary to mutations in other genes, such as *Apc*. It is possible that differences in these and other biological markers in tumors that appear histologically similar are indications of the mutational history of the tumor and the pathway by which they arose, rather than defining a difference in tumor type.

The higher tumor incidence and multiplicity in male $Mlh1^{-/-}$ mice parallels the increased CRC risk in men with Lynch

syndrome[58] with both environmental and genetic causes proposed.[59] Sensitivity to DSS-induced inflammation and radiation-induced intestinal cell apoptosis have also been shown to differ by sex,[60–62] although the mechanisms are not well understood.

In conclusion, our results indicate a potential for exposure to ionizing radiation to further increase the progression of preneoplastic lesions in *Mlh1*$^{-/-}$ mice with inflammatory colitis. Given the coalition of radiogenic mutation, MMR-deficiency, and inflammatory processes, the tumors arising following such combined exposures are likely to exhibit a complex series of traits rather than recapitulating any single human CRC subtype. Comprehensive genetic analysis in the future may be able reveal more information about the specific interactions between the various exposures. In the meantime, these results are in agreement with the principle that signs of inflammation should be closely monitored in MMR-deficient patients, such as those with Lynch syndrome, before exposure to radiation for therapy, diagnostic, or screening purposes.

Acknowledgements

This work was supported in part by the Ministry of Education, Culture, Sports, Science, and Technology (Kakenhi) (Grant No. 22501009).

Disclosure Statement

The authors have no conflict of interest.

References

1 Lichtenstein P, Holm NV, Verkasalo PK *et al.* Environmental and heritable factors in the causation of cancer–analyses of cohorts of twins from Sweden, Denmark, and Finland. *N Engl J Med* 2000; **343**: 78–85.
2 United Nations, Sources and Effects of Ionizing Radiation. United Nations Scientific Committee on the Effects of Atomic Radiation, 2000 report to general Assembly, with Scientific Annexes, United Nations Sales publication E.00, IX.4 New York, United Nations. 2000.
3 International Commission on Radiological Protection. ICRP Publication 79. Genetic Susceptibility to Cancer, Annals of the ICRP, 1998.
4 Ferlay J, Shin HR, Bray F, Forman D, Mathers C, Parkin DM. Estimates of worldwide burden of cancer in 2008: GLOBOCAN 2008. *Int J Cancer* 2010; **127**: 2893–917.
5 de la Chapelle A. Genetic predisposition to colorectal cancer. *Nat Rev Cancer* 2004; **4**: 769–80.
6 Mecklin JP. Frequency of hereditary colorectal carcinoma. *Gastroenterology* 1987; **93**: 1021–5.
7 Ponz de Leon M, Sassatelli R, Sacchetti C, Zanghieri G, Scalmati A, Roncucci L. Familial aggregation of tumors in the three-year experience of a population-based colorectal cancer registry. *Cancer Res* 1989; **49**: 4344–8.
8 Kunkel TA, Erie DA. DNA mismatch repair. *Annu Rev Biochem* 2005; **74**: 681–710.
9 Schofield MJ, Hsieh P. DNA mismatch repair: molecular mechanisms and biological function. *Annu Rev Microbiol* 2003; **57**: 579–608.
10 Modrich P, Lahue R. Mismatch repair in replication fidelity, genetic recombination, and cancer biology. *Annu Rev Biochem* 1996; **65**: 101–33.
11 Silva FC, Valentin MD, Ferreira Fde O, Carraro DM, Rossi BM. Mismatch repair genes in Lynch syndrome: a review. *Sao Paulo Med J* 2009; **127**: 46–51.
12 Coussens LM, Werb Z. Inflammation and cancer. *Nature* 2002; **420**: 860–7.
13 Kaser A, Zeissig S, Blumberg RS. Inflammatory bowel disease. *Annu Rev Immunol* 2010; **28**: 573–621.
14 Kohonen-Corish MR, Daniel JJ, te Riele H, Buffinton GD, Dahlstrom JE. Susceptibility of *Msh2*-deficient mice to inflammation-associated colorectal tumors. *Cancer Res* 2002; **62**: 2092–7.
15 Taniguchi K, Kakinuma S, Tokairin Y *et al.* Mild inflammation accelerates colon carcinogenesis in *Mlh1*-deficient mice. *Oncology* 2006; **71**: 124–30.
16 Fujiwara I, Yashiro M, Kubo N, Maeda K, Hirakawa K. Ulcerative colitis-associated colorectal cancer is frequently associated with the microsatellite instability pathway. *Dis Colon Rectum* 2008; **51**: 1387–94.
17 Suzuki H, Harpaz N, Tarmin L *et al.* Microsatellite instability in ulcerative colitis-associated colorectal dysplasias and cancers. *Cancer Res* 1994; **54**: 4841–4.
18 Fleisher AS, Esteller M, Harpaz N *et al.* Microsatellite instability in inflammatory bowel disease-associated neoplastic lesions is associated with hypermethylation and diminished expression of the DNA mismatch repair gene, hMLH1. *Cancer Res* 2000; **60**: 4864–8.
19 Ozasa K, Shimizu Y, Suyama A *et al.* Studies of the mortality of atomic bomb survivors, Report 14, 1950-2003: an overview of cancer and noncancer diseases. *Radiat Res* 2012; **177**: 229–43.
20 Margel D, Baniel J, Wasserberg N, Bar-Chana M, Yossepowitch O. Radiation therapy for prostate cancer increases the risk of subsequent rectal cancer. *Ann Surg* 2011; **254**: 947–50.
21 Rodriguez AM, Kuo YF, Goodwin JS. Risk of colorectal cancer among long-term cervical cancer survivors. *Med Oncol* 2014; **31**: 943.
22 Martin LM, Marples B, Coffey M *et al.* DNA mismatch repair and the DNA damage response to ionizing radiation: making sense of apparently conflicting data. *Cancer Treat Rev* 2010; **36**: 518–27.
23 Xu XS, Narayanan L, Dunklee B, Liskay RM, Glazer PM. Hypermutability to ionizing radiation in mismatch repair-deficient, *Pms2* knockout mice. *Cancer Res* 2001; **61**: 3775–80.
24 Tokairin Y, Kakinuma S, Arai M *et al.* Accelerated growth of intestinal tumours after radiation exposure in *Mlh1*-knockout mice: evaluation of the late effect of radiation on a mouse model of HNPCC. *Int J Exp Pathol* 2006; **87**: 89–99.
25 Baker SM, Plug AW, Prolla TA *et al.* Involvement of mouse *Mlh1* in DNA mismatch repair and meiotic crossing over. *Nat Genet* 1996; **13**: 336–42.
26 Cooper HS, Murthy S, Kido K, Yoshitake H, Flanigan A. Dysplasia and cancer in the dextran sulfate sodium mouse colitis model. Relevance to colitis-associated neoplasia in the human: a study of histopathology, B-catenin and p53 expression and the role of inflammation. *Carcinogenesis* 2000; **21**: 757–68.
27 Cooper HS, Murthy SN, Shah RS, Sedergran DJ. Clinicopathologic study of dextran sulfate sodium experimental murine colitis. *Lab Invest* 1993; **69**: 238–49.
28 Okayasu I, Yamada M, Mikami T, Yoshida T, Kanno J, Ohkusa T. Dysplasia and carcinoma development in a repeated dextran sulfate sodium-induced colitis model. *J Gastroenterol Hepatol* 2002; **17**: 1078–83.
29 Okamoto M, Yonekawa H. Intestinal tumorigenesis in Min mice is enhanced by X-irradiation in an age-dependent manner. *J Radiat Res (Tokyo)* 2005; **46**: 83–91.
30 Boivin GP, Washington K, Yang K *et al.* Pathology of mouse models of intestinal cancer: consensus report and recommendations. *Gastroenterology* 2003; **124**: 762–77.
31 Pascal RR. Dysplasia and early carcinoma in inflammatory bowel disease and colorectal adenomas. *Hum Pathol* 1994; **25**: 1160–71.
32 Riddell RH, Goldman H, Ransohoff DF *et al.* Dysplasia in inflammatory bowel disease: standardized classification with provisional clinical applications. *Hum Pathol* 1983; **14**: 931–68.
33 Chen WG, Chen YY, Kamel OW, Koo CH, Weiss LM. p53 mutations in Hodgkin's disease. *Lab Invest* 1996; **75**: 519–27.
34 Sakurai N, Iwamoto S, Miura Y *et al.* Novel p53 splicing site mutation in Li-Fraumeni-like syndrome with osteosarcoma. *Pediatr Int* 2013; **55**: 107–11.
35 Jolly KW, Malkin D, Douglass EC, Brown TF, Sinclair AE, Look AT. Splice-site mutation of the p53 gene in a family with hereditary breast-ovarian cancer. *Oncogene* 1994; **9**: 97–102.
36 Magnusson KP, Sandstrom M, Stahlberg M *et al.* p53 splice acceptor site mutation and increased HsRAD51 protein expression in Bloom's syndrome GM1492 fibroblasts. *Gene* 2000; **246**: 247–54.
37 Neufert C, Becker C, Neurath MF. An inducible mouse model of colon carcinogenesis for the analysis of sporadic and inflammation-driven tumor progression. *Nat Protoc* 2007; **2**: 1998–2004.
38 Tanaka T, Kohno H, Suzuki R, Yamada Y, Sugie S, Mori H. A novel inflammation-related mouse colon carcinogenesis model induced by azoxymethane and dextran sodium sulfate. *Cancer Sci* 2003; **94**: 965–73.
39 Karin M, Greten FR. NF-kappaB: linking inflammation and immunity to cancer development and progression. *Nat Rev Immunol* 2005; **5**: 749–59.
40 Ishizuka S, Ito S, Onuma M, Kasai T, Aoyama Y, Hara H. Ingestion of sugar beet fiber enhances irradiation-induced aberrant crypt foci in the rat

colon under an apoptosis-suppressed condition. *Carcinogenesis* 1999; **20**: 1005–9.
41 Zhang Y, Rohde LH, Emami K *et al.* Suppressed expression of non-DSB repair genes inhibits gamma-radiation-induced cytogenetic repair and cell cycle arrest. *DNA Repair (Amst)* 2008; **7**: 1835–45.
42 Gatalica Z, Torlakovic E. Pathology of the hereditary colorectal carcinoma. *Fam Cancer* 2008; **7**: 15–26.
43 Clarke AR. Studying the consequences of immediate loss of gene function in the intestine: APC. *Biochem Soc Trans* 2005; **33**: 665–6.
44 Sehgal R, Sheahan K, O'Connell PR, Hanly AM, Martin ST, Winter DC. Lynch syndrome: an updated review. *Genes (Basel)* 2014; **5**: 497–507.
45 Hussain SP, Amstad P, Raja K *et al.* Increased p53 mutation load in noncancerous colon tissue from ulcerative colitis: a cancer-prone chronic inflammatory disease. *Cancer Res* 2000; **60**: 3333–7.
46 Itzkowitz SH, Yio X. Inflammation and cancer IV. Colorectal cancer in inflammatory bowel disease: the role of inflammation. *Am J Physiol Gastrointest Liver Physiol* 2004; **287**: G7–17.
47 Brenner H, Kloor M, Pox CP. Colorectal cancer. *Lancet* 2014; **383**: 1490–502.
48 Torlakovic EE, Gomez JD, Driman DK *et al.* Sessile serrated adenoma (SSA) vs. traditional serrated adenoma (TSA). *Am J Surg Pathol* 2008; **32**: 21–9.
49 Snover DC. Update on the serrated pathway to colorectal carcinoma. *Hum Pathol* 2011; **42**: 1–10.
50 Jass JR, Stewart SM, Stewart J, Lane MR. Hereditary non-polyposis colorectal cancer–morphologies, genes and mutations. *Mutat Res* 1994; **310**: 125–33.
51 Alexander J, Watanabe T, Wu TT, Rashid A, Li S, Hamilton SR. Histopathological identification of colon cancer with microsatellite instability. *Am J Pathol* 2001; **158**: 527–35.
52 Greenson JK, Bonner JD, Ben-Yzhak O *et al.* Phenotype of microsatellite unstable colorectal carcinomas: Well-differentiated and focally mucinous tumors and the absence of dirty necrosis correlate with microsatellite instability. *Am J Surg Pathol* 2003; **27**: 563–70.
53 Jenkins MA, Hayashi S, O'Shea AM *et al.* Pathology features in Bethesda guidelines predict colorectal cancer microsatellite instability: a population-based study. *Gastroenterology* 2007; **133**: 48–56.
54 Young J, Simms LA, Biden KG *et al.* Features of colorectal cancers with high-level microsatellite instability occurring in familial and sporadic settings: parallel pathways of tumorigenesis. *Am J Pathol* 2001; **159**: 2107–16.
55 Jass JR. Pathology of hereditary nonpolyposis colorectal cancer. *Ann N Y Acad Sci* 2000; **910**: 62–73; discussion -4.
56 Mecklin JP, Sipponen P, Jarvinen HJ. Histopathology of colorectal carcinomas and adenomas in cancer family syndrome. *Dis Colon Rectum* 1986; **29**: 849–53.
57 Andersen SH, Lykke E, Folker MB, Bernstein I, Holck S. Sessile serrated polyps of the colorectum are rare in patients with Lynch syndrome and in familial colorectal cancer families. *Fam Cancer* 2008; **7**: 157–62.
58 Aarnio M, Sankila R, Pukkala E *et al.* Cancer risk in mutation carriers of DNA-mismatch-repair genes. *Int J Cancer* 1999; **81**: 214–8.
59 Dunlop MG, Farrington SM, Carothers AD *et al.* Cancer risk associated with germline DNA mismatch repair gene mutations. *Hum Mol Genet* 1997; **6**: 105–10.
60 Berglund M, Thomas JA, Fredin MF, Melgar S, Hornquist EH, Hultgren OH. Gender dependent importance of IRAK-1 in dextran sulfate sodium induced colitis. *Cell Immunol* 2009; **259**: 27–32.
61 Tanaka T, Morishita Y, Kawamori T *et al.* Synergistic effect of radiation on colon carcinogenesis induced by methylazoxymethanol acetate in ACI/N rats. *Jpn J Cancer Res* 1993; **84**: 1031–6.
62 Weil MM, Xia C, Xia X, Gu X, Amos CI, Mason KA. A chromosome 15 quantitative trait locus controls levels of radiation-induced jejunal crypt cell apoptosis in mice. *Genomics* 2001; **72**: 73–7.